

Scaling Human Cancer Risks from Low LET to High LET when Dose-Effect Relationships are Complex

Authors: Shuryak, Igor, Fornace, Albert J., Datta, Kamal, Suman, Shubhankar, Kumar, Santosh, et al.

Source: Radiation Research, 187(4) : 486-492

Published By: Radiation Research Society

URL: <https://doi.org/10.1667/RR009CC.1>

The BioOne Digital Library (<https://bioone.org/>) provides worldwide distribution for more than 580 journals and eBooks from BioOne's community of over 150 nonprofit societies, research institutions, and university presses in the biological, ecological, and environmental sciences. The BioOne Digital Library encompasses the flagship aggregation BioOne Complete (<https://bioone.org/subscribe>), the BioOne Complete Archive (<https://bioone.org/archive>), and the BioOne eBooks program offerings ESA eBook Collection (<https://bioone.org/esa-ebooks>) and CSIRO Publishing BioSelect Collection (<https://bioone.org/csiro-ebooks>).

Your use of this PDF, the BioOne Digital Library, and all posted and associated content indicates your acceptance of BioOne's Terms of Use, available at www.bioone.org/terms-of-use.

Usage of BioOne Digital Library content is strictly limited to personal, educational, and non-commercial use. Commercial inquiries or rights and permissions requests should be directed to the individual publisher as copyright holder.

BioOne is an innovative nonprofit that sees sustainable scholarly publishing as an inherently collaborative enterprise connecting authors, nonprofit publishers, academic institutions, research libraries, and research funders in the common goal of maximizing access to critical research.

Scaling Human Cancer Risks from Low LET to High LET when Dose-Effect Relationships are Complex

Igor Shuryak,^{a,1} Albert J. Fornace Jr.,^b Kamal Datta,^b Shubhankar Suman,^b Santosh Kumar,^b Rainer K. Sachs^c and David J. Brenner^a

^a Center for Radiological Research, Columbia University, New York, New York; ^b Department of Biochemistry and Molecular and Cellular Biology, and Lombardi Comprehensive Cancer Center, Georgetown University, Washington DC; and ^c Departments of Mathematics and Physics, University of California, Berkeley, California

Shuryak, I., Fornace, A. J. Jr., Datta, K., Suman, S., Kumar, S., Sachs, R. K. and Brenner, D. J. Scaling Human Cancer Risks from Low LET to High LET when Dose-Effect Relationships are Complex. *Radiat. Res.* 187, 486–492 (2017).

Health risks from space radiations, particularly from densely ionizing radiations, represent an important challenge for long-ranged manned space missions. Reliable methods are needed for scaling low-LET to high-LET radiation risks for humans, based on animal or *in vitro* studies comparing these radiations. The current standard metric, relative biological effectiveness (RBE) compares iso-effect doses of two radiations. By contrast, a proposed new metric, radiation effects ratio (RER), compares effects of two radiations at the same dose. This definition of RER allows direct scaling of low-LET to high-LET radiation risks in humans at the dose or doses of interest. By contrast to RBE, RER can be used without need for detailed information about dose response shapes for compared radiations. This property of RER allows animal carcinogenesis experiments to be simplified by reducing the number of tested radiation doses. For simple linear dose-effect relationships, $RBE = RER$. However, for more complex dose-effect relationships, such as those with nontargeted effects at low doses, RER can be lower than RBE. We estimated RBE and RER values and uncertainties using heavy ion (¹²C, ²⁸Si, ⁵⁶Fe) and gamma-ray-induced tumors in a mouse model for intestinal cancer (APC^{1638N/+}), and used both RBE and RER to estimate low-LET to high-LET risk scaling factors. The data showed clear evidence of nontargeted effects at low doses. In situations, such as the ones discussed here where nontargeted effects dominate at low doses, RER was lower than RBE by factors around 2.8–3.5 at 0.03 Gy and 1.3–1.4 at 0.3 Gy. It follows that low-dose high-LET human cancer risks scaled from low-LET human risks using RBE may be correspondingly overestimated. © 2017 by Radiation Research Society

¹ Address for correspondence: Center for Radiological Research, Columbia University Medical Center, 630 West 168th St., VC-11-235, New York, NY 10032; email: is144@cumc.columbia.edu.

INTRODUCTION

Long-distance/long-duration trips such as a Mars mission are expected to expose astronauts to densely ionizing high-LET radiations in the dose range totaling 0.3–0.5 Gy or more (1, 2). These high-LET radiations consist of a wide variety of charged particles as well as neutrons, all with a broad range of energies. Human data quantifying high-LET radiation risks are very limited; consequently, to reliably estimate human health risks from space mission exposures it is necessary to appropriately scale the much better known low-LET (gamma ray or X ray) radiation risks to estimate high-LET heavy ion risks in humans.

Low-LET to high-LET scaling is typically based on experimental studies of radiation-induced carcinogenesis in mice (or other pertinent endpoints), sometimes augmented by corresponding *in vitro* studies, induced by gamma rays and appropriate high-LET radiations (3). The standard approach to analyzing such studies is to produce low-LET to high-LET scaling factors using the concept of relative biological effectiveness (RBE) (4, 5). RBE is defined as the ratio of doses of the two compared radiations (e.g. low and high LET) that will produce equal biological effects (3). This iso-effect-based RBE concept was introduced in 1931 by Failla and Henshaw (6) in the context of radiotherapy, to correct for the different biological effectiveness of X rays vs. gamma rays in producing either tumor control or radiation-induced side effects.

Since 1931, this iso-effect approach has been universally used to quantify the difference in biological effect between two types of radiation. While this approach is appropriate in a radiotherapeutic context where the goal is indeed to achieve equal effects of one radiation vs. another, it is less clear that this approach is optimal in the context of risk estimation for one radiation relative to another, where iso-effect is not directly relevant.

The goal of the current study is to investigate optimal methods for scaling low-LET to high-LET radiation-induced cancer risks. As we discuss below, when the dose-response relationships are simple, for example linear

with dose, there are no significant issues, and estimating an appropriate scaling factor based on *in vivo* or *in vitro* laboratory data is, at least in principle, simple to perform. However, it is now reasonably well established that dose-response relationships for radiation-induced cancer are not simple, for example potentially reflecting a saturating dose-response relationship at low doses, perhaps due to nontargeted effects, then a linear or upwardly curving linear-quadratic response at intermediate doses, and then a downwardly curving dose response at higher doses, perhaps reflecting the effects of cell killing.

These different mechanisms typically result in a complex nonlinear dose-response relationship. In such cases, there are meaningfully different possible approaches toward estimating low-LET to high-LET cancer risk scaling factors, only one of which is use of RBE. As we show, these different approaches can result in numerically different estimated low-LET to high-LET cancer risk scaling factors, even when the same data set is used, and would thus result in different high-LET cancer risk estimates in humans.

To investigate alternative approaches to estimating low-LET to high-LET scaling factors in the context of a complex dose-response relationship, we use here a mechanistically motivated cancer risk model to analyze the carcinogenic effectiveness of heavy ions and gamma rays within a murine carcinogenesis data set. To estimate scaling factors from gamma rays to heavy ions we used: 1. the standard RBE approach; and 2. a new metric – the radiation effects ratio (RER) at a given dose.

MATERIALS AND METHODS

Mouse Carcinogenesis Data Set

The data set analyzed was radiation-induced intestinal tumorigenesis in APC^{1638N/+} mice, as previously reported by Suman *et al.* (7). Male mice (females were also used in the experimental study, but for illustrative purposes we analyzed the male data only because they showed more tumors) were exposed at age 6 to 8 weeks to ¹²C ions (doses: 0.1, 0.5 and 2.0 Gy; energy: 290 MeV/n; LET: 13 keV/μm), ²⁸Si ions (doses: 0.1, 0.5 and 1.4 Gy; energy: 300 MeV/n; LET: 69 keV/μm) and ⁵⁶Fe ions (doses: 0.1, 0.5 and 1.6 Gy; energy: 1000 MeV/n; LET: 148 keV/μm) at the NASA Space Radiation Laboratory (NSRL) at Brookhaven National Laboratory. Mice were also exposed to gamma rays (0.1, 0.5, 1 and 2 Gy) using a ¹³⁷Cs source and control mice were sham irradiated. Twenty mice were used per radiation type/dose.

Radiation-Dose-Response Model

The main assumptions of the radiation-dose-response model used here were described in previous publications (8, 9), as well as by other groups (10). The HZE-ion fluences, which produce the doses relevant for anticipated space missions are relatively low, and therefore many cell nuclei will not be directly “hit” during the mission (11). Those which are hit, especially by ion track cores, can suffer severe DNA damage: e.g., complex and difficult to repair double-strand breaks. Such damage, often referred to as targeted effects, can kill cells or potentially transform them into a premalignant state (8, 9).

In addition, signals can be propagated from cells that were directly hit to nonhit bystander neighbor cells, resulting in these bystander cells potentially being switched to a stressed or “activated” state, and

increasing the probability of these cells ultimately being transformed into a premalignant state (8, 9). These processes are often referred to as nontargeted or bystander effects (8–10).

Based on these concepts, we can write the mean number of tumors per mouse $M(d)$ at radiation dose d as:

$$M(d) = (c_1 + c_2 \times (1 - \exp[-c_3 \times d]) + c_4 \times d) \times \exp[-c_5 \times d] \quad (1)$$

Here parameter c_1 is the background tumor incidence. Parameter c_2 is the maximum excess tumor incidence due to nontargeted effects. In other words, the nontargeted effects contribution saturates to this value at high doses. Parameter c_3 is the dose-response slope (exponential) for nontargeted effects: it determines how quickly the nontargeted effects contribution approaches c_2 as dose increases. Parameter c_4 is the dose-response slope for tumor induction by targeted effects. Parameter c_5 relates to radiation-induced cell killing (i.e., cytotoxic effects).

Quadratic terms for tumor induction can in principle also be added to the model. The same can be done to cell killing by introducing a quadratic term into the exponential relationship so that the cell survival probability becomes determined by the commonly used linear-quadratic formalism. We performed preliminary calculations on the data using a model version which included quadratic terms for both tumor induction and cell killing, but these calculations showed that the presence of such terms was not supported by the current data set. Consequently, we proceeded with the analyses described below using the model described in Eq. (1), which is similar to the model used by Chang *et al.* (10) in analyzing murine Harderian gland tumorigenesis by various high-LET radiations.

The error distribution around the mean $M(d)$ from Eq. (1) was assumed (12) to be negative binomial (NB). Thus, $P_{NB}(k)$, the probability of observing k tumors in a mouse, can be written as

$$P_{NB}(k) = (1/[r \times Q])^{1/r} \times (M(d)/Q)^k \times \Gamma(k + 1/r) / [\Gamma(1/r) \times k!], \quad (2)$$

where $Q = M(d) + 1/r$, Γ is the gamma function and r is the “overdispersion” parameter. If $r \sim 0$, there is no overdispersion and the variance and mean are equal, as in the Poisson distribution. On the other hand, if $r > 0$, then the variance becomes greater than the mean and the ratio of variance to mean increases as the mean increases.

Metrics for Comparing the Effects of Different Radiation Types: RBE and RER

The RBE is defined as the ratio of iso-effective doses for gamma rays vs. heavy ions (3, 6). In the context of radiation carcinogenesis, RBE is the ratio of doses of two different radiations, which result in equivalent excess tumor yields, as schematized in Fig. 1A. RBE is easily interpretable, it has a long history of use (3, 6), and it is convenient to use for simple dose responses such as linear or linear quadratic. When radiation effects saturate at high doses or decrease due to cell killing, RBE is sometimes impossible to calculate (Fig. 1A) because no gamma-ray dose (not even a large one) can produce an effect of the same magnitude as a given high-LET dose.

Alternatively, as schematized in Fig. 1B, a measure of the relative effectiveness for carcinogenesis by two different radiations can be generated by comparing the mean excess (i.e. radiation induced) tumors per exposed animal for one radiation vs. the other, *at the same radiation dose*. The key difference between this concept, which we term the radiation effects ratio, and the classical RBE is that the RER compares the effects of the two radiations at the same radiation dose. Thus, if the measured mean number of tumors at dose d is $M(d)$, and the (zero dose) control value is c_1 , then the RER for ion I, relative to gamma rays, is defined as:

$$\text{RER}_I = [M_I(d) - c_1] / [M_\gamma(d) - c_1] \quad (3)$$

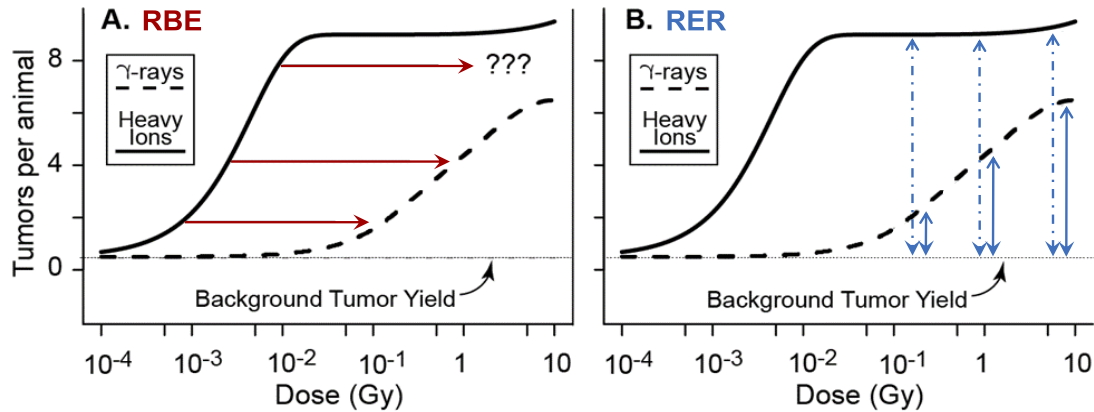


FIG. 1. Schematic comparison of two metrics for evaluating radiation effects: relative biological effectiveness (RBE, panel A) and radiation effects ratio (RER, panel B). The dose responses for tumors per animal from heavy ions (solid curves) and gamma rays (dashed curves) are hypothetical. As described in the main text, calculation of RBE involves a “horizontal” comparison of dose responses (arrows in panel A) to identify a gamma-ray dose which has the same effect as the selected heavy-ion dose. RBE is the ratio of iso-effective gamma-ray and heavy-ion doses. In some cases, (question marks in panel A) there may be no solution for RBE. By contrast, calculation of RER involves a “vertical” comparison of excess tumor yields from heavy ions and gamma rays (dashed vs. solid arrows in panel B) at the same dose.

The motivation for RER is similar to that of epidemiological radiation-effect metrics like excess relative risk [ERR; e.g., ref. (13)]; here the effects of different radiation types are “vertically” compared at the same radiation dose (Fig. 1B). This new approach is qualitatively distinct from RBE, which involves a “horizontal” comparison of iso-effective doses (Fig. 1A). RER can be estimated for any dose-response shape, even when dose-responses saturate (Fig. 1B) or turn downwards due to cell killing.

RESULTS

Graphical comparison of the model [Eq. (1)] fits and the data for intestinal tumor yields per mouse are shown in Fig. 2. The estimated model parameter values and uncertainties are shown in Table 1.

As shown in Fig. 2, the best-fit dose responses for the heavy ions, but not gamma rays, rose steeply in the dose region below 0.1 Gy and then at larger doses their slopes decreased. In the context of our model [Eq. (1)], nontargeted effects were the cause of this steep initial rise of the heavy-ion dose responses.

To assess whether inclusion of the nontargeted effects mechanisms was statistically justified on the basis of the data, we compared the fits for the full model [Eq. (1)] and for the reduced model without the nontargeted effects component [i.e., with $c_2 = 0$ in Eq. (1)] using the standard Akaike information criterion approach (AICc) adjusted for sample size (14). AICc values for the tested models were converted into strength of evidence values called Akaike weights (14); larger Akaike weights indicate higher support from the data. In the case analyzed here, the Akaike weights for the model without nontargeted effects were 0.881, 0.266, 0.007 and 0.014 for gamma rays, ^{12}C ions, ^{28}Si ions and ^{56}Fe ions, respectively. Consequently, the targeted-effects-only model (i.e., without nontargeted effects) had very high support for gamma rays, weaker support for ^{12}C ions and very low support for ^{28}Si and ^{56}Fe ions. Thus, a

comparatively complex model for the heavy-ion dose response, i.e., including nontargeted effects, is supported by the HZE-ion data, a conclusion also reached by Chang *et al.* (10) analyzing heavy-ion-induced Harderian gland tumorigenesis.

The best-fit overdispersion parameter (r) was larger than zero for all tested ions, but could not be distinguished from zero with confidence for gamma rays (Table 1). In other words, the errors around the gamma ray data were consistent with the Poisson distribution, but for heavy ions an overdispersed negative binomial distribution produced better fits. This information allows more realistic uncertainties to be calculated for ion-induced effects (see below), compared with the commonly-used assumption of a Poisson distribution of tumors induced by all radiation types.

Based on the model fits summarized in Fig. 2 and Table 1, estimated RBE and RER values and corresponding 95% confidence intervals for each ion vs. gamma rays are shown in Fig. 3 and Table 2. The high RBE and RER values for all tested ions at low doses were caused by nontargeted effects, which were important for heavy ions, but not for gamma rays. Both RBE and RER values were highest for ^{28}Si and ^{56}Fe ions relative to carbon ions, and the effectiveness ordering of $^{28}\text{Si} > ^{56}\text{Fe} > ^{12}\text{C}$ was the same for both RBE and RER.

Figure 4 shows the ratio of RBE to RER values for the three studied ions. Because of the different shapes of the high-LET vs. low-LET dose-response curves in the current analysis, the estimated RER values were lower than estimated RBE values. These different RER values relative to RBE values directly translate into correspondingly different factors for scaling low-LET risks to high-LET risks, and thus correspondingly different high-LET human risk estimates.

It may be noted from Fig. 3 and Table 2 that the confidence intervals associated with the RER estimates are generally wider than those associated with the RBE

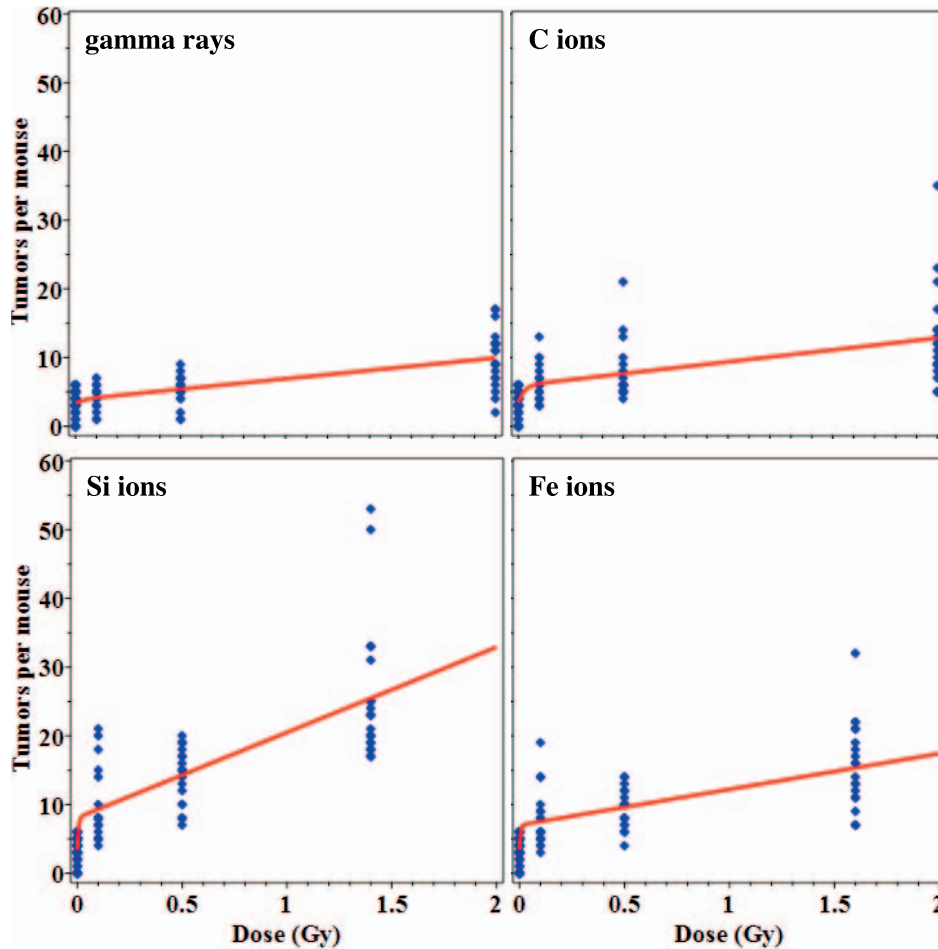


FIG. 2. Comparison of data (symbols) and model best fits (curves). Each symbol represents the number of intestinal tumors detected in an individual mouse.

estimates. Essentially this is because the experimental design of the original study was to optimize RBE estimates. As discussed below, an experimental design with the same number of mice but optimized for RER estimates would result in much narrower confidence limits for the RER estimates than the current design.

As an example of the application of RBE and RER based scaling metrics, we used the RBE and RER estimates calculated here (Table 2 and Fig. 3) based on mouse data to generate lifetime colon cancer risk estimates for a 40-year-

old astronaut exposed, for example, to silicon ions. The low-LET-gamma-ray lifetime risks were derived from the National Cancer Institute's Radiation Risk Assessment Tool (RADRAT) (15), which implements models developed in the biological effects of ionizing radiation (BEIR VII report) (16). We multiplied the RADRAT low-LET risk estimates by the estimated RBE or RER values for ^{28}Si ions (Table 2 and Fig. 3) and propagated the corresponding relative errors to generate RBE-based and RER-based risk estimates and confidence limits for the ^{28}Si ions.

TABLE 1
Best-Fit Model Parameter Values and 95% Confidence Intervals (CI)

Model parameter	Gamma rays (95% CI)	C ions (95% CI)	Si ions (95% CI)	Fe ions (95% CI)
Background tumors/mouse (c_1)	3.40 (3.00, 3.87)	3.40 (2.91, 3.87)	3.40 (2.91, 3.87)	3.40 (3.00, 3.87)
Maximum excess tumors/mouse from nontargeted effects (c_2)	0.48 (0.0, ∞)	2.52 (0.59, 3.66)	4.70 (2.71, 6.32)	3.62 (1.76, 5.07)
Dose-response slope for nontargeted effects (c_3 , Gy^{-1})	25.79 (0.0, ∞)	36.82 (3.64, ∞)	222.47 (7.21, ∞)	222.34 (6.98, ∞)
Dose-response slope for targeted effects (c_4 , tumors/mouse/Gy)	3.03 (0.01, 9.48)	3.47 (2.09, 13.92)	12.41 (9.46, 26.98)	5.20 (3.49, 16.49)
Cell killing (c_5 , Gy^{-1})	0.0 (0.0, 0.0)	0.0 (0.0, 0.0)	0.0 (0.0, 0.0)	0.0 (0.0, 0.0)
Over-dispersion parameter (r)	0.026 (0.0, 0.094)	0.093 (0.045, 0.164)	0.073 (0.037, 0.128)	0.057 (0.018, 0.116)

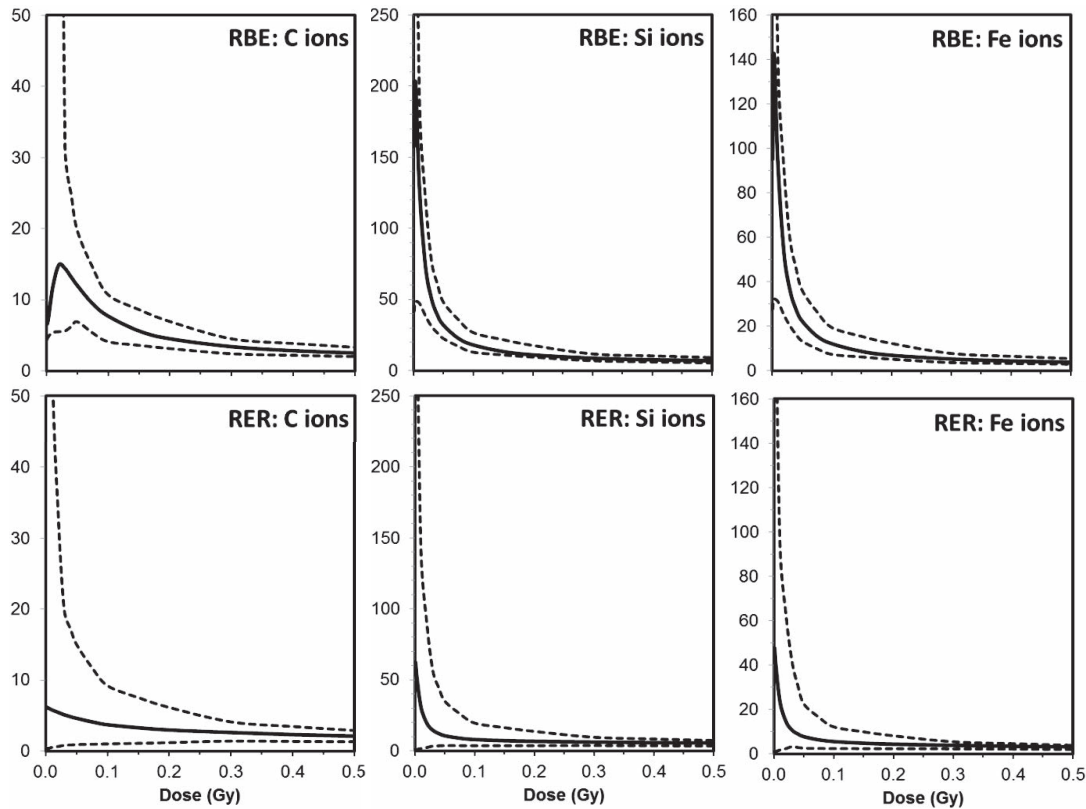


FIG. 3. RBE and RER estimates (solid curves) and 95% confidence limits (dashed curves), as function of radiation dose and radiation type.

In this particular example (though not of course in general) we are applying scaling information from mouse intestinal tumors to human colon cancers. The APC^{1638N/+} mutant mouse is a well-established model for human colorectal cancer (17–19) and, in this case, both the order of tumorigenic effectiveness per unit dose as well as the dose-response shapes were similar for the mutant mouse intestinal vs. colon tumors (7).

The lifetime human colon cancer risk estimates are shown in Fig. 5, as scaled from human gamma-ray risks using both RBE and RER; upper 95% confidence limits are also shown. Because the RER estimates are smaller than the corresponding RBE estimates (Table 2 and Fig. 4), the estimated lifetime risks as estimated with the RER methodology are correspondingly smaller than those estimated using the RBE methodology.

TABLE 2
Ion- and Dose-Dependent RBE and RER Estimates and 95% Confidence Limits (CI)

Dose (Gy)	RBE for C ions			RBE for Si ions			RBE for Fe ions		
	95% CIs			95% CIs			95% CIs		
0.01	11.7	5.4	847.3	126.6	47.2	188.3	92.4	31.0	138.9
0.03	14.4	5.6	31.4	50.5	31.1	76.9	36.2	20.1	59.1
0.05	12.0	6.9	19.7	32.0	22.5	48.0	22.4	13.3	36.3
0.10	7.7	4.1	10.7	18.0	12.9	26.7	12.1	7.3	19.4
0.30	3.4	2.4	4.5	8.7	6.9	11.7	5.2	3.6	7.7
0.50	2.5	2.0	3.3	6.9	5.4	9.2	3.8	2.9	5.4
Dose (Gy)	RER for C ions			RER for Si ions			RER for Fe ions		
	95% CIs			95% CIs			95% CIs		
0.01	5.8	0.5	57.2	30.8	1.6	141.6	23.4	1.7	94.0
0.03	5.1	0.8	19.8	14.4	3.3	56.0	10.7	3.2	41.7
0.05	4.6	0.9	15.0	10.6	3.6	34.9	7.7	2.5	22.4
0.10	3.7	1.0	9.2	7.9	3.5	19.5	5.5	2.3	12.1
0.30	2.6	1.4	4.1	6.1	3.6	9.5	3.8	2.2	5.4
0.50	2.1	1.3	2.9	5.5	3.4	7.2	3.1	1.9	3.8

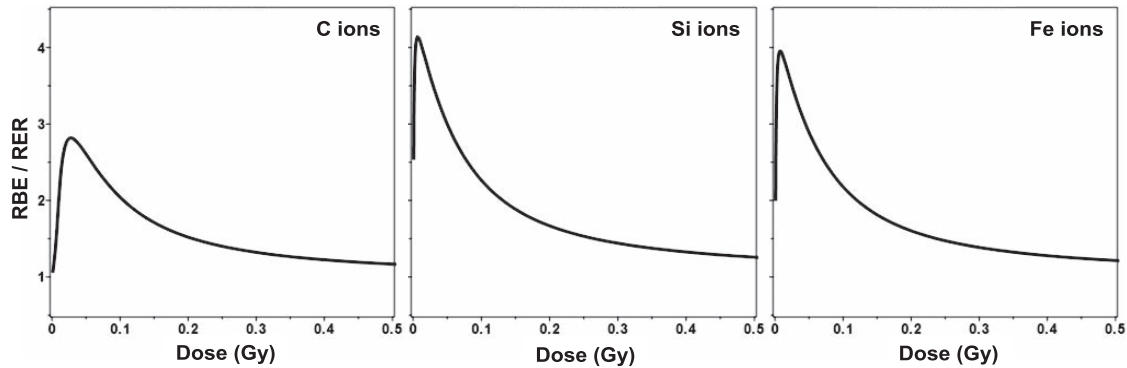


FIG. 4. Estimates of RBE/RER ratios as function of radiation dose and radiation type.

DISCUSSION

The goal of this study was to investigate different methods to use laboratory-based radiation-induced carcinogenesis data for scaling gamma-ray risks to human heavy-ion-radiation risks, at doses relevant for long-distance manned space missions (1, 2). While the methodologies are obvious for simple (e.g. linear) dose-effect relationships, this is not so when the dose-effect relationship is complex. For example, for dose responses involving both targeted effects and nontargeted effects the appropriate methodologies are less clear.

As the input to this study we conducted a mechanistically motivated quantitative analysis of heavy-ion- and gamma-ray-induced intestinal carcinogenesis in a transgenic mouse system. Our dose-response model, which was used for data analysis, includes targeted effects and nontargeted effects for radiation-induced tumors; it was indeed complex in

shape, with a rapid increase in radiation response at low doses (<0.1 Gy) due to nontargeted effects, followed by a slower increase at higher doses. We calculated conventional RBE values for the tested ions, and developed and applied a new methodology, RER, describing a different low-LET to high-LET scaling approach.

As shown in Fig. 1, RBE involves a “horizontal scaling” of high-LET vs. low-LET doses that result in the same level of risk. By contrast (see Fig. 1), RER involves a “vertical” scaling of high-LET vs. low-LET radiation-induced risks at the same dose. Because RER is defined as the ratio of radiation-induced tumors at the same dose, it allows direct scaling of low-LET to high-LET radiation risks at the dose of interest. Consequently, we expect that application of RER should, at least in principle, result in more accurate estimation of high-LET heavy-ion risks as compared with RBE.

The relationship between RER and RBE is of course determined by the shapes of the dose-response relationships for the high-LET and low-LET radiations. For example, consider the simple case where the dose responses for heavy ions and for gamma rays are linear; then $RER = RBE$. Now consider a scenario where cell killing causes the dose responses for both tested radiations to decrease at high doses; here RER and RBE are not equivalent often $RER < RBE$, given biologically plausible parameter values. A realistic low-dose scenario studied in this work is where the heavy-ion dose response has a dominant nontargeted response at low doses around and below 0.1 Gy; in this case $RER < RBE$ (Fig. 4). As the dose increases and the relative significance of the nonlinear-nontargeted response diminishes, the difference between RER and RBE correspondingly decreases (Fig. 4).

Radiation effects ratio also has a number of practical advantages as compared with RBE. For example, the use of RER can lead to a more efficient experimental design for laboratory studies motivated to generate low-LET- to high-LET-risk scaling factors. Specifically, an experimental design motivated by RBE estimation requires the estimation of the shapes of dose-response relationships to identify iso-effective doses; such an experimental design requires acquiring data at a number of radiation doses. By contrast,

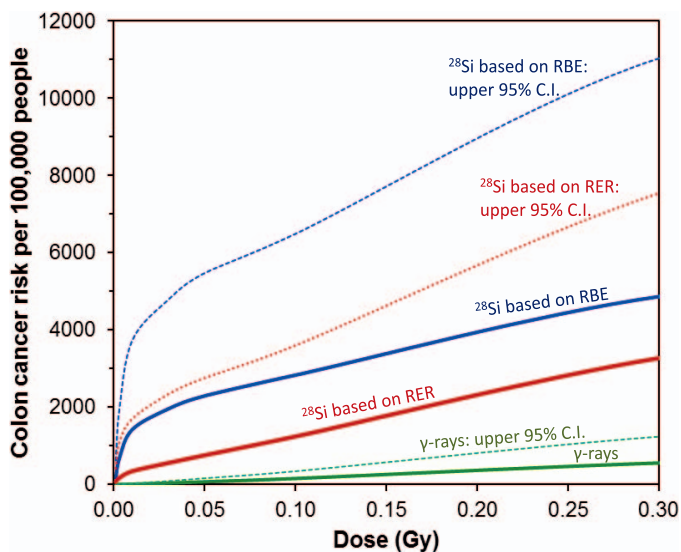


FIG. 5. Estimated lifetime ^{28}Si -ion-induced colon cancer risk for a 40-year-old individual (sex averaged). Lifetime colon cancer risks induced by gamma rays (solid green curve) were estimated as described in the text and scaled to ^{28}Si ions based on RBE (solid blue curve) or based on RER (solid red curve). Dashed curves represent upper 95% confidence limits.

the use of RER requires only a single gamma-ray data point at the same dose as the high-LET data point of interest.

Thus, instead of measuring heavy-ion and gamma-ray effects at multiple doses to characterize dose-response shapes for subsequent RBE estimation, it may be sufficient to measure the effects only at one dose point in the heavy-ion dose range of interest and to estimate RER there. Resources could therefore be concentrated to study a specific heavy ion dose range and RER values calculated in this range could then be used to transfer radiation-induced risks from animals to humans.

Finally, it is pertinent to point out, as shown in Fig. 3 and Table 2, that the uncertainty bounds surrounding the RER estimates are somewhat wider than those surrounding the corresponding RBE estimates, even though the underlying data set was the same for both estimates. To an extent, this is a function of the design of the experimental mouse study (7), which was optimized for RBE estimation. Thus, for example in the ^{28}Si ion experiment, 20 mice were used for each of the four heavy-ion doses and the four gamma-ray doses, a total of 160 animals. The use of four doses was motivated by the requirement to estimate iso-effect doses. If, by contrast, a RER at (say) 0.1 Gy was the goal, then the same (160) mouse resources could be allocated as 80 mice at 0.1 Gy (^{28}Si ions) and 80 mice at 0.1 Gy (gamma rays). Simulating the results of this experimental design using the data from our analysis, the width of the 95% confidence interval of the RER estimate could be reduced by a factor of two.

In summary, the definition of RER potentially allows direct scaling of radiation-induced risks from gamma rays to heavy ions at any dose of interest (Fig. 1). This definition of low-LET to high-LET scaling factors is qualitatively and often numerically different from the classical RBE approach which assesses iso-effect doses. We have argued here that low-dose high-LET human cancer risk estimates based on scaling with RER are likely to be more accurate than those based on RBE.

In situations such as the ones discussed here, where nontargeted effects dominate the dose response at low doses, RER can be less than RBE at these doses by factors ranging of approximately 2.8–3.5 at 0.03 Gy and approximately 1.3–1.4 at 0.3 Gy. It follows that low-dose high-LET human cancer risk estimates as scaled from low-LET human risks using RBE may be correspondingly overestimated.

ACKNOWLEDGMENTS

This study was supported NASA Grants NNX15AI21G and NNX16AR81A. Stimulating discussions with Dr. Steven Blattnig and colleagues at the NASA Langley Research Center are gratefully acknowledged.

Accepted: January 15, 2017; published online: February 20, 2017

REFERENCES

1. Durante M. Space radiation protection: Destination Mars. *Life Sci Space Res (Amst)* 2014; 1:2–9.
2. Kim M-HY, Rusek A, Cucinotta FA. Issues for simulation of galactic cosmic ray exposures for radiobiological research at ground-based accelerators. *Front Oncol* 2015; 5:122.
3. NCRP. National Council on Radiation Protection and Measurements. The relative biological effectiveness of radiations of different quality. NCRP Report 104; 1990.
4. Cucinotta FA. Biophysics of NASA radiation quality factors. *Radiat Prot Dosimetry* 2015; 166(1-4):282–9.
5. Cucinotta FA. Review of NASA approach to space radiation risk assessments for Mars exploration. *Health Phys* 2015; 108(2): 131–42.
6. Failla G, Henshaw PS. The relative biological effectiveness of X rays and gamma rays. *Radiol Management* 1931; 17:1–43.
7. Suman S, Kumar S, Moon BH, Strawn SJ, Thakor H, Fan Z, et al. Relative biological effectiveness of energetic heavy ions for intestinal tumorigenesis shows male preponderance and radiation type and energy dependence in APC(1638N/+) mice. *Int J Radiat Oncol Biol Phys* 2016; 95(1):131–8.
8. Shuryak I, Brenner DJ, Ullrich RL. Radiation-induced carcinogenesis: mechanistically based differences between gamma rays and neutrons, and interactions with DMBA. *Plos One* 2011; 6(12): e28559.
9. Shuryak I, Sachs RK, Brenner DJ. Biophysical models of radiation bystander effects: 1. Spatial effects in three-dimensional tissues. *Radiat Res* 2007; 168(6):741–9.
10. Chang PY, Cucinotta FA, Bjornstad KA, Bakke J, Rosen CJ, Du N, et al. Harderian gland tumorigenesis: low-dose and LET response. *Radiat Res* 2016; 185(5):449–60.
11. Cacao E, Hada M, Saganti PB, George KA, Cucinotta FA. Relative biological effectiveness of HZE particles for chromosomal exchanges and other surrogate cancer risk endpoints. *PLoS One* 2016; 11(4):e0153998.
12. Payne EH, Hardin JW, Egede LE, Ramakrishnan V, Selassie A, Gebregziabher M. Approaches for dealing with various sources of overdispersion in modeling count data: Scale adjustment versus modeling. *Stat Meth Med Res* 2015; 0962280215588569.
13. Thompson DE, Mabuchi K, Ron E, Soda M, Tokunaga M, Ochikubo S, et al. Cancer incidence in atomic bomb survivors. Part II: Solid tumors, 1958-1987. *Radiat Res* 1994; 137(2 Suppl): S17–67.
14. Burnham KP, Anderson DR. Model selection and multi-model inference: A practical information-theoretic approach: Springer Verlag, New York; 2002.
15. Berrington de Gonzalez A, Iulian Apostoaei A, Veiga LH, Rajaraman P, Thomas BA, Owen Hoffman F, et al. RadRAT: a radiation risk assessment tool for lifetime cancer risk projection. *J Radiol Prot* 2012; 32(3):205–22.
16. NRC. Health Risks from Exposure to Low Levels of Ionizing Radiation - BEIR VII. Washington, DC: The National Academies Press, Washington DC; 2006.
17. Taketo MM. Mouse models of gastrointestinal tumors. *Cancer Sci* 2006; 97(5):355–61.
18. Grady WM, Markowitz SD. Genetic and epigenetic alterations in colon cancer. *Annu Rev Genomics Hum Genet* 2002; 3:101–28.
19. Suman S, Fornace Jr AJ, Datta K. Animal models of colorectal cancer in chemoprevention and therapeutics development: INTECH Open Access Publisher; 2012.